ORIENTAL JOURNAL OF CHEMISTRY
An International Open Access, Peer Reviewed Research Journal
www.orientjchem.org
ISSN: 0970-020 X
CODEN: OJCHEG
2025, Vol. 41, No.(6):
Pg. 1863-1872

Structural Characterization and *In-silico* Evaluation of Bioactive Compounds from *Neisosperma oppositifolium* Leaves as Anti-diabetic and Anti-cancer agents

RAMUDU POTHURAJU[1], SUSMITHA AGGARAPU[1]*, PRAMOD KUMAR MERIGA[1,2], POOJA BANDI[1], GIREESH KUMAR ERI[1] and SWARNALATHA DUGASANI[1]

[1]*Annamacharya College of Pharmacy, Rajampet-516126, Andhra Pradesh, India.
[2]JNTUA Oil Technological and Pharmaceutical Research Institute, Ananthapuramu-515002, Andhra Pradesh, India.
*Corresponding author E-mail: aggarapusuma@gmail.com

http://dx.doi.org/10.13005/ojc/410602

(Received: June 09, 2025; Accepted: November 22, 2025)

ABSTRACT

Present study aimed to isolate, characterize, and evaluate the pharmacological activity of phytoconstituents from the ethanolic leaf extract of *Neisosperma oppositifolium*, a medicinal plant known for its ethnopharmacological relevance. Dried leaves were subjected to maceration using ethanol, and phytochemical screening revealed the presence of indole alkaloids, which were further separated and purified through thin layer and column chromatography. Three major compounds, coded as NO-1, NO-2, and NO-3, were isolated and subjected to characterization using attenuated total reflectance-fourier transform infrared spectroscopy, proton and carbon-13 nuclear magnetic resonance, and electrospray ionization mass spectrometry. Molecular docking studies against target proteins 2JJK for anti-diabetic and 3KOK for anti-cancer revealed binding energies ranging from –7.4 to –6.5 kcal/mol for diabetic targets and –6.0 to –5.6 kcal/mol for cancer targets, with Compound NO-1 and NO-2 showing the highest affinities and favorable interactions. This integrative study not only elucidated the chemical identity of bioactive compounds in *N. oppositifolium* but also provided predictive evidence for their pharmacological potential in managing diabetes and cancer.

Keywords: *Neisosperma oppositifolium*, Indole alkaloids, Maceration, Structural characterization, Molecular docking, PASS prediction.

INTRODUCTION

The exploration of natural products from medicinal plants continues to play a vital role in the discovery of novel therapeutic agents[1]. The most challenging and prevalent global health issues of the 21st century are Diabetes mellitus and cancer[2]. As per the reports of International Diabetes Federation[3], over 530 million people worldwide were living with diabetes in 2023, and this figure is expected to rise significantly due to factors such as sedentary lifestyles, obesity, and unhealthy dietary habits[4]. Among them, nearly 90% of cases accounts for Type 2 or non-insulin dependent

diabetes, which is characterized by impaired glucose metabolism due to insulin resistance[5]. According to the World Health Organisation (WHO), there will be around 10 million cancer-related deaths and 20 million new cancer cases worldwide in 2026, making cancer a major source of morbidity and mortality[6]. Both diseases impose substantial burdens on healthcare systems and economies. Interestingly, a growing body of evidence suggests a bidirectional link between diabetes and certain types of cancer, due to shared risk factors like chronic inflammation, hyperinsulinemia, and oxidative stress[7,8]. Despite advances in treatment, limitations such as drug resistance, adverse effects, and high costs necessitate the exploration of safer, plant-derived therapeutic alternatives[9].

Indole alkaloids are a structurally diverse group of natural metabolites with wideranging distribution across various biological sources. They exhibit a broad spectrum of pharmacological effects, including antibacterial, antimalarial, anti-inflammatory, antiviral, and anticancer activities[10]. Their chemical diversity and multifaceted therapeutic potential have positioned indole alkaloids as important scaffolds in natural productbased drug discovery, particularly in the areas of diabetes management and cancer treatment. For example, vindoline[11], tetrahydroalstonine[12], and reserpine[13] display promising antidiabetic effects by improving insulin sensitivity, regulating glucose metabolism, and inhibiting carbohydrate-hydrolyzing enzymes. Compounds such as vincristine[14], vinblastine[15], and evodiamine[16] are either firmly established as chemotherapeutics or exhibit strong anticancer potential by inducing apoptosis, suppressing cell growth, inhibiting angiogenesis, and interfering with microtubule dynamics.

In this context, the investigation of natural bioactive compounds with dual anti-diabetic and anti-cancer activity holds significant potential for the development of novel and more effective therapeutic agents[17]. In recent years, the integration of phytochemical analysis with computational drug discovery tools has accelerated the identification of bioactive compounds and their potential biological targets[18].

No prior scientific studies on the biological activities or chemical constituents of selected plant Neisosperma oppositifoliumhave been documented in the available literature. In light of this research gap, the current study was undertaken to explore the pharmacological potential of its bioactive compounds. This involved a systematic approach of extraction, isolation, analytical characterization, and biological evaluation, with a focus on predicting anti-diabetic and anti-cancer activities through in silico methods[19-21]. The study aims to provide a foundational understanding of the plant's therapeutic potential and support further pharmacological investigations.

Plant Profile

Neisosperma oppositifolium, commonly known astonga, tokelau, and aikikiru, belongs to Apocynaceae family and is traditionally recognized for its management in diabetes and hypertension. The biological source is the dried leaves, which are rich in indole alkaloids such as bleekerine, ochropposinine, isorespilline, and 3-epirauvanine. The plant typically grows as a small to moderate tree reaching up to 15m in height and exudes latex. It is widely distributed throughout the South Pacific and extends westward into the Indian ocean, thriving in littoral forests, mangrove swamp edges, and limestone-rich environments. The plant typically flowers during summer, followed shortly by fruiting.

MATERIALS AND METHODS

Instrumentsand Chemicals

Various instruments and Software tools used for the study were single-pan electronic weighing balance (Axis LC/GC), UV chamber (Medimeas, Ambala), ATR-FTIR spectrophotometer (Alpha II Bruker), NMR spectrophotometer (Bruker 500 MHz), ESI MS (G3540A-Agilent 8890) and PASS online and AutoDock 4.2 for *in silico* prediction of biological activity. Several chemicals and solvents viz ethanol, methanol, petroleum ether, hexane, chloroform, toluene, ethyl acetate, and various acids used were of laboratory-grade and all sourced from Molychem, Mumbai.

Plant Collection and authentication

To prepare various solvents extracts, fresh and healthy leaves of *Neisosperma oppositifolium* (Fig.1) wereprocured from Dwaraka medicinal garden, located in Gangireddy Palli village, Yerraguntla, Kadapa District, A.P., India. The authentication of this plant was authorized by botanist from Government Degree college, Rajampet, Annamayya District, A.P., India.

Fig. 1. Fresh and dried leaves of *Neisosperma oppositifolium*

Extraction of constituents

Freshly collected leaves were thoroughly washed with water to remove dust particles and shade-dried at room temperature for 10 days (Fig. 1). The dried material was ground into a fine powder, and 50 g of this powder was macerated in 250 ml of different solvents of increasing polarities viz., *n*-hexane, toluene, chloroform, ethyl acetate, ethanol, methanol, and waterfor 7 days. After maceration, the extracts were filtered and concentrated under reduced pressure using a rotary evaporator. The total weight of crude extracts were 0.542, 0.683, 0.751, 0.824, 0.967, 0.934, and 0.926 g, with the percentage yields of 0.01, 0.013, 0.015, 0.016, 0.019, 0.018, and 0.018%, respectively.

Phytochemical analysis

It was performed on all extracts to identify the presence of major phytoconstituent groups. Tests for alkaloids, glycosides, tannins, and flavonoids were performed using standard protocols.[22] These tests helped in selecting the most promising extract for further isolation and characterization.

Chromatographic analysis

Ethanolic leaf extract of *N. oppositifolium* was analysed through chromatography[23] to isolate and purify bioactive constituents, particularly indole alkaloids. TLC was performed initially for the preliminary separation and optimization of solvent system. Silica gel based TLC plates containing a fluorescent dye were activated at 110°C for 30 min and developed using various freshly prepared solvent systems as shown in Table 1. Crude extracts and isolated compounds were spotted on the TLC plates, and chromatograms were developed using saturated chambers, visualized under UV light at 254 nm and 365 nm, and R_f values were computed for analysis. Based on the TLC results, the solvent system vizn-hexane: methanol:ethyl acetate: water (3:1:5:1) was given clear and well-resolved bands, making it suitable for bulk separation via column chromatography. A silica gel-packed column (60–120 mesh) was used as the stationary phase, and polarity was gradually increased to optimize elution. Fractions were collected, monitored using TLC, and those showing similar profiles were pooled, concentrated, and subjected to spectroscopic characterization and in silico biological evaluation.

Table 1: Various mobile phase compositions employed for TLC Studies

Sr. No	Mobile Phase	Composition
1	Methanol: water	2:8
2	Ethyl acetate: methanol	8:2
3	n-Butanol:water: glacial acetic acid	4:1:5
4	Ethyl acetate: methanol: triethylamine	8:2
5	Toluene:ethyl acetate:formic acid	7:2:1
6	n-hexane: methanol:ethyl acetate: water	3:1:5:1

Analytical characterization by Spectroscopic analysis

The concentrated fractions obtained were labelled as A, B, C, D, E and F. upon phytochemical analysis, fractions D, E, F tested positive for indole alkaloids. Then they were concentrated and subjected to characterization using ATR-FTIR, ^{1}H and ^{13}C-NMR and ESI-MS[24] to elucidate their molecular structures. The combined spectral analysis resulted in identification of functional groups, structural and molecular mass of phytochemical constituents present in these fractions.

***In-silico* Evaluation of Pharmacological activity**

The Prediction of Activity Spectra for Substances (PASS) online tool was used to evaluate possible biological activities based on structureactivity relationships, with activities having Pa values>0.5 considered potentially significant[25]. To further explore their pharmacological potential, molecular docking studies were conducted using AutoDock software (ver. 4.2) to estimate binding affinities against two therapeutically validated and clinically relevant target proteins. 2JJK, Human fructose-1,6-bisphosphatase, a key enzyme in gluconeogenesis and a validated antidiabetic target[26], as its inhibition lowers glucose production without causing hypoglycemia or weight gain, and 3KOK, a central signaling mediator in cell growth and survival, and an established target for anticancer therapy[27], were chosen as clinically relevant protein targets for *in-silico* bioactivity evaluation against diabetes and cancer.

The docking scores, expressed as binding energy (ΔG, kcal/mol), reflect the strength of interaction between each compound and the active site of the respective proteins[28]. Lower (more negative) binding energy values indicate stronger binding affinity, suggesting potential biological relevance. The number of hydrogen bonds and key interacting residues were also analysed to gain insights into the binding mode[29].

RESULTS AND DISCUSSION

Phytochemical screening of ethanolic extract (0.967 g) of *N. oppositifolium* leaves given a positive result for indole alkaloids, which were well resolvedthrough the optimization of n-hexane: methanol:ethyl acetate: water (3:1:5:1v/v) as the mobile phase and purified through thin layer and column chromatography respectively. The purified fractions that showed positive for indole alkaloids were coded as compound NO-1, NO-2 and NO-3and subjected to characterization using advanced spectroscopic techniques.

Analytical Characterization

Characterization of isolated compound was established using ATR-FTIR, ^{1}H, ^{13}C NMR and mass spectrometry and spectral data are presented below:

Compound NO-1: Pale yellow liquid; Thalleoquine test-negative, vitali-morin test-negative, Van urk's test-positive; R_f-0.64 (solvent: *n*-hexane: methanol:ethyl acetate: water (3:1:5:1v/v); ATR-FTIR cm^{-1}: 3408.66, N–H str. (Secondary amide); 1712.47, C=O str. (Ester carbonyl); 1642.12, C=O str. (Amide carbonyl); 1260.98, C–O str. (Methoxy group); 1149.47, C–O–C str. (Cyclic ether)(Fig. 2a); ^{1}H NMR (Acetone d_6, 400 MHz), δH 3.73 (6H, singlet, OCH_3), 3.81 (3H, singlet, OCH_3), 9.25 (1H, singlet, NH) 1.16-1.18 (3H, doublet, CH_3), 6.33 (1H, doublet, Aromatic), 6.83 (1H, doublet, Aromatic), 7.25-7.27 (^{1}H, doublet, Aromatic), 1.64-1.78 (2H, multiplet, CH_2), 1.88-1.95 (1H, multiplet, CH_2), 2.05-2.11 (1H, multiplet, CH), 2.27-2.30 (1H, multiplet, CH), 2.40-2.47 (1H, multiplet, CH_2), 2.91-3.01 (5H, multiplet, CH_2 & CH), 4.76-4.81 (1H, multiplet, CH)(Fig. 3a); ^{13}C NMR (101 MHz, Acetone d_6), δC 201.88(1C), 167.82(1C), 157.32(1C), 150.36 (1C), 145.32(1C), 141.09 (1C), 132.21(1C), 117.98(1C), 104.70(1C), 70.73(1C), 65.54 (1C), 61.26 (1C), 55.23 (1C), 53.07(1C), 46.23(2C), 29.82 (1C), 13.85 (1C) (Fig. 4a); ESI-MS(m/z): 429.20 ($[M+H]^+$) for $C_{23}H_{26}N_2O_6$ (Figure 5a).

Compound NO-2: Pale yellow liquid; Thalleoquine test-negative, vitali-morin test-negative, Van urk's test-positive; R_f-0.64 (solvent: *n*-hexane: methanol:ethyl acetate: water (3:1:5:1v/v); ATR-FTIR cm^{-1}: 3363.92, N–H str. (indole); 2941.24, C-H str. (sp^3); 1711.78, C=O str. (ester); 1243.98, C–O str. (Methoxy or ester group); 1149.95/1098/1037, C–N or C–O str. (amine or ether), 851.55/799/ 755.10, Aromatic C–H bending (out-of-plane)(Fig. 2b); ^{1}H NMR (Acetone d_6, 400 MHz), δH 3.59 (6H, singlet, OCH_3), 3.74 (3H, singlet, OCH_3), 9.25 (1H, singlet, NH) 1.17-1.18 (3H, doublet, CH_3), 4.60-4.65 (1H, doublet, Aromatic), 6.32-6.38 (1H, doublet, Aromatic), 7.27-7.29 (1H, doublet, Aromatic), 1.88-2.26 (2H, multiplet, CH_2), 2.58-2.68 (1H, multiplet, CH_2), 2.75-2.88 (1H, multiplet, CH), 2.90-2.92 (1H, multiplet, CH), 2.95-3.01 (5H, multiplet, CH_2 & CH), 4.20-4.23 (1H, multiplet, CH)(Fig. 3b); ^{13}C NMR (101 MHz, Acetone d_6), δC 162.40 (1C), 149.70 (1C), 149.30 (1C), 143.50 (1C), 136.90 (1C), 134.50 (1C), 127.05 (1C),

122.60 (1C), 108.12 (2C), 94.80 (1C), 70.86 (1C), 59.85 (1C), 56.16 (1C), 52.25 (1C), 39.20 (2C), 38.20 (1C), 31.80 (1C), 21.60 (1C), 18.10 (1C)(Fig. 4b); ESI-MS(m/z): 413.20 ($[M+H]^+$) for $C_{23}H_{26}N_2O_6$ (Figure 5b).

Compound NO-3: Pale yellow liquid; Thalleoquine test-negative, vitali-morin test-negative, Van urk's test- positive; R_f-0.68 (solvent: *n*-hexane: methanol:ethyl acetate: water (3:1:5:1v/v); ATR-FTIR cm^{-1}: 3589.45, 3498.13, O–H str. (broad, strong); 2985.82, 2939.20, 2913.16, C-H str. (sp^3, aliphatic); 1712.49, C=O str. (strong); 1642.91, C=C or C=N str.; 1412.96, 1364.14, C-H bending (CH_2, CH_3); 1244.66, 1149.43, C–O str. (ether); 1037.73, C–N or C–O str. (amine or ether), 934.54/856.34, Aromatic indole C–H bending (out-of-plane); 755.94, Ring deformation/aromatic substitution band (Fig. 2c); ^{1}H NMR (Acetone d_6, 400 MHz), δH 3.54 (6H, singlet, OCH_3), 3.60 (3H, singlet, OCH_3), 9.51 (1H, singlet, NH) 1.39-1.45 (3H, doublet, CH_3), 5.48 (1H, doublet, Aromatic), 6.32-6.38 (1H, doublet, Aromatic), 1.91-1.99 (2H, multiplet, CH_2), 2.08-2.13 (1H, multiplet, CH_2), 2.17 (1H, multiplet, CH), 2.23-2.97 (1H, multiplet, CH), 3.34-3.39 (5H, multiplet, CH_2& CH), 4.14-4.18 (1H, multiplet, CH) (Fig. 3c); ^{13}C NMR (101 MHz, Acetone d_6), δC 208.50 (1C), 149.30 (1C), 136.90 (1C), 134.50 (1C), 127.05 (1C), 108.12 (2C), 94.80 (1C), 60.20 (1C), 59.15 (1C), 56.16 (2C), 52.60 (1C), 46.00 (1C), 40.20 (1C), 35.90 (1C), 33.31 (1C), 27.94 (1C) 21.60 (1C) (Fig. 4c); ESI-MS(m/z): 373.21 ($[M+H]^+$) for $C_{23}H_{26}N_2O_6$ (Figure 5c).

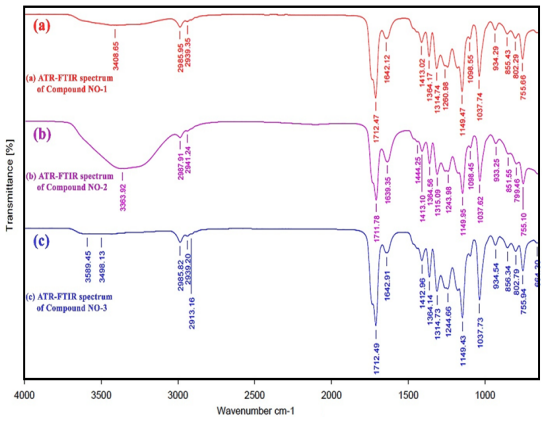

Fig. 2. ATR-FTIR spectra of (a) Compound NO-1 (b) Compound NO-2 (c) Compound NO-3

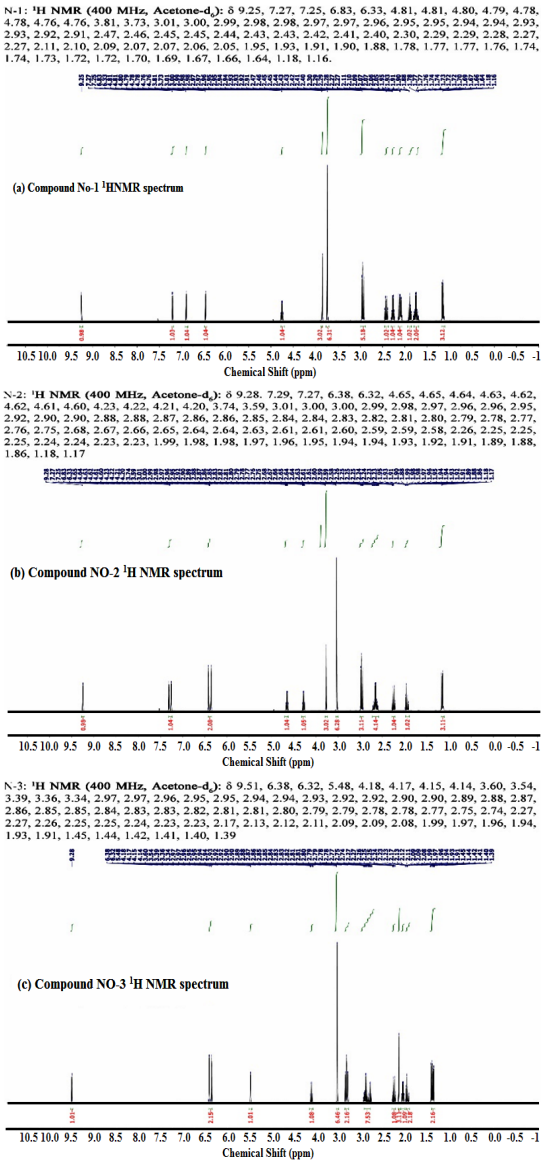

Fig. 3. ^{1}H NMR spectra of (a) Compound NO-1 (b) Compound NO-2 (c) Compound NO-3

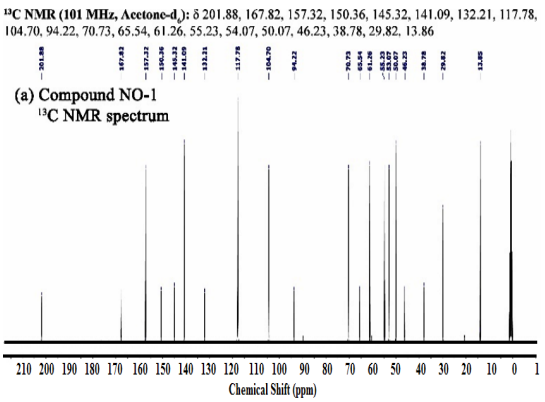

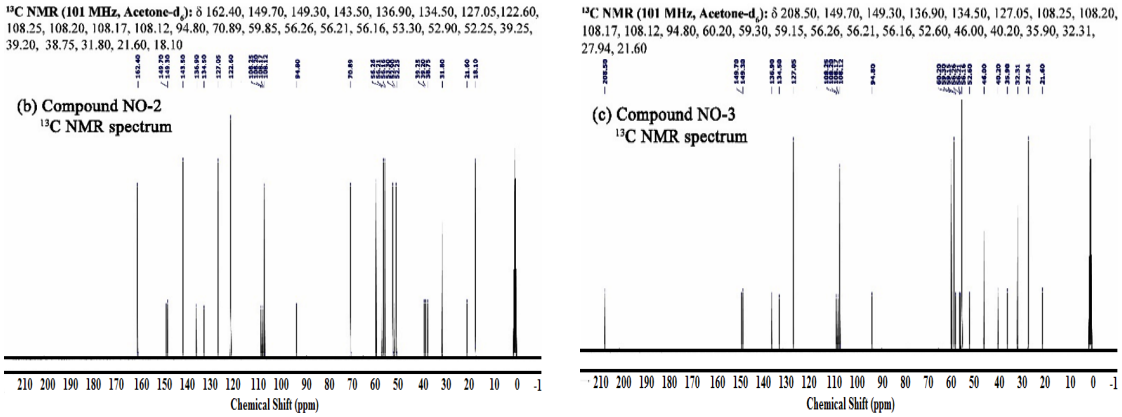

Fig. 4. ^{13}C NMR spectra of (a) Compound NO-1 (b) Compound NO-2 (c) Compound NO-3

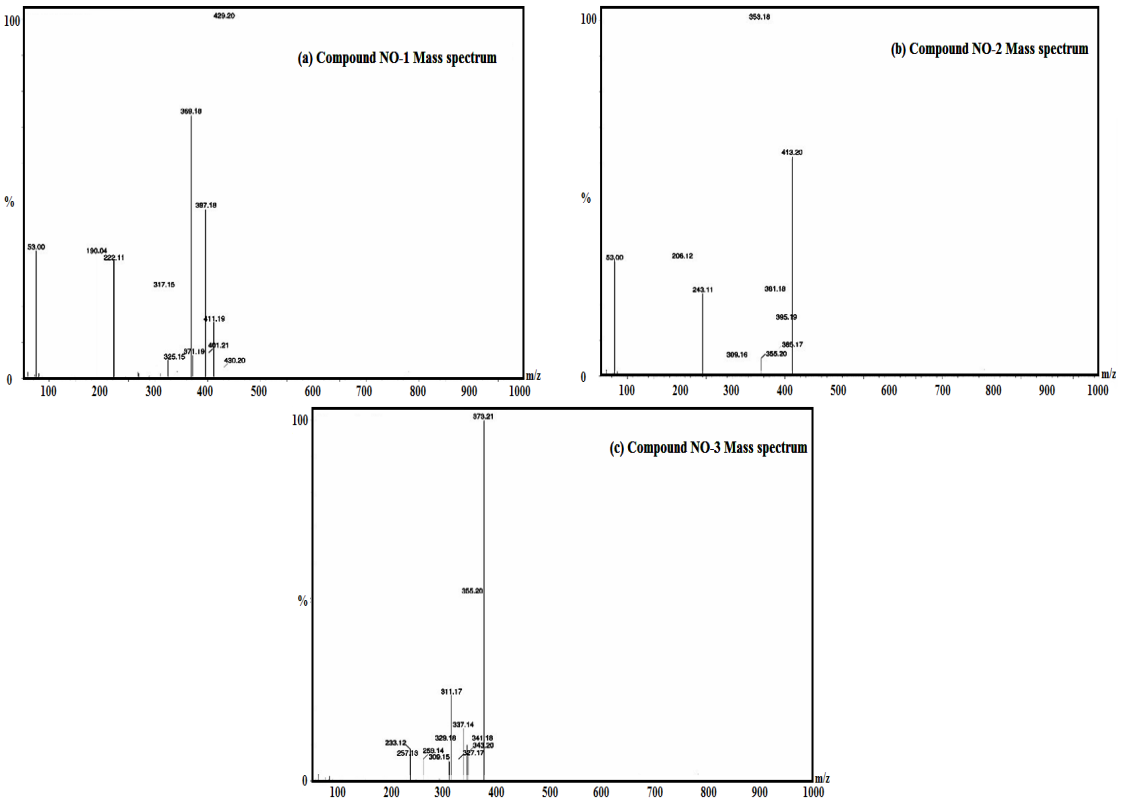

Fig. 5. Mass spectra of (a) Compound NO-1 (b) Compound NO-2 (c) Compound NO-3

After spectral interpretation, Compound NO-1, NO-2, NO-3 were identified as Methyl 5,6-dimethoxy-1'-methyl-2-oxa-4a',5',5a',7',8',10a'-hexahydro-1'H,10'H-spiro[indoline-3,6'-pyrano[3,4-f]indolizine]-3'-carboxylate with a chemical formula of $C_{23}H_{26}N_2O_6$ (428 g/mol) (Fig. 6a), Methyl 10,11-dimethoxy-4-methyl-4a,5,7,8,13,13b,14,14a-octahydro-4H-indolo[2,3-a] pyrano[3,4-g]quinolizine-2-carboxylate with a chemical formula of $C_{23}H_{26}N_2O_6$, (412.47 g/mol) (Fig. 6b) and 1-(3-(2-Hydroxyethyl)-9,10-dimethoxy-1,2,3,4,6,7,12,12b-octahydroindolo[2,3-a]quinolizin-2-yl)ethan-1-one with a chemical formula of $C_{23}H_{26}N_2O_6$(372 g/mol) respectively (Figure 6c).

The comparison of the three compounds with reported analogues in the chemical database, PubChem, indicates that NO-2 is closely related to a compound called Reserpiline (PubChem CID 67228)30 and Isoreserpiline (PubChem CID 161345)[31], which share the same class of

indolo-pyranoquinolizine alkaloids with similar substitutions and core structure, suggesting a known type of indole alkaloid derivative and NO-3 aligns well with Corynantheidine (PubChem CID 6540753)[32], which has an indoloquinolizine core with similar methoxy and hydroxyethyl substitutions, supporting structural validation as related to known indoloquinolizine alkaloids.while NO-1 may represent a novel spiro structure combining indoline and pyranoindolizine moieties.

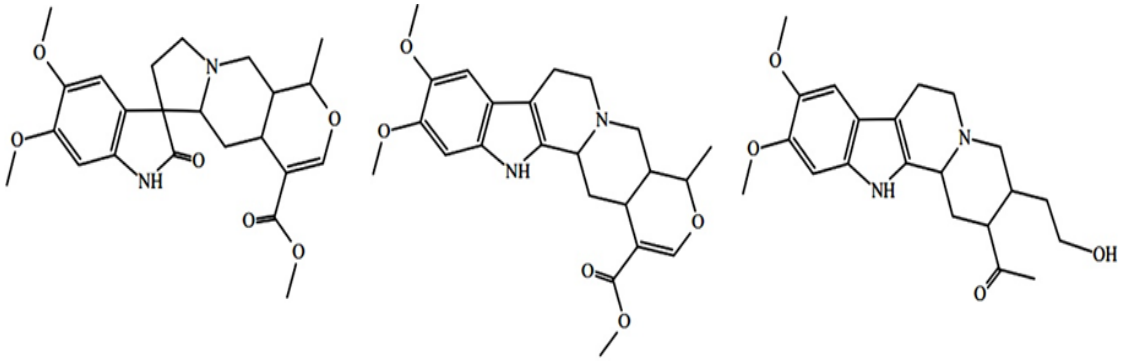

Fig. 6. Predicted structures of (a) Compound NO-1 (b) Compound NO-2 (c) Compound NO-3

In silico biological evaluation

Prediction using PASS online tool

Based on structureactivity relationships, The probable biological activity of the isolated compounds (NO-1, NO-2 and NO-3) from ethanolic extract of *N. oppositifolium* was predictedusing the PASS online tool. The three compounds NO-1, NO-2, NO-3 showed anti-diabetic and anti-cancer activities with Pa and Pi values as indicated in Table 2.

Table 2: PASS prediction results of isolated compounds

Compound ID	Predicted Activity	Pa (Probability Active)	Pi (Probability Inactive)
NO-1	Anti-diabetic	0.701	0.010
	Anti-cancer	0.608	0.043
NO-2	Anti-diabetic	0.727	0.057
	Anti-cancer	0.589	0.021
NO-3	Anti-diabetic	0.688	0.015
	Anti-cancer	0.615	0.018

Molecular docking analysis

All three isolated compounds demonstrated distinct binding affinities against diabetic (2JJK) and anticancer (3KOK) targets. Each compound's binding energy provides insight into its relative interaction strength with both target proteins. NO-1 exhibited the strongest antidiabetic effect, while NO-2 displayed superior anticancer binding. Binding energies and interacting with key residues involved in substrate recognition and activity modulation are shown in Table 3 and Fig. 8 & Figure 9.

Table 3: Comparative docking results

Compound	Target Protein	Binding Energy (kcal/mol)	Key interacting residues	Comparative Potential
NO-1	2JJK	- 7.4	GlyA18, GlyC18, ThrC19, GlyA20, MetC10, ArgA14, ArgC14	Most effective antidiabetic
NO-2	2JJK	- 6.8	Arg C14, Met A10, Arg C17, Gly A18, Arg A14	Moderate antidiabetic interaction
NO-3	2JJK	- 6.5	Met C160, Ala C16, Val C9, Leu C26, Glu C12, Gly C13, Leu C22, Arg C123, Arg C17	Weak antidiabetic interaction
Acarbose	2JJK	- 6.5	GlyA20, ArgA14, ThrC19	Reference antidiabetic standard
NO-1	3KOK	- 5.8	Val A93, Arg A51, Leu A191	Moderate anticancer interaction
NO-2	3KOK	- 6.0	ValA92, ArgA51, ThrA52, LysA54, LeuA53	Highest anticancer potential
NO-3	3KOK	- 5.6	Arg A51, Val A93, Thr A52, Leu A53, Lys A54	Weak anticancer interaction
Imatinib	3KOK	- 6.5	LysA54, ValA92, ArgA51	Reference anticancer standard

For the diabetic target protein 2JJK, standard inhibitors such as acarbose[33] generally show binding affinities in the range of –6.5 kcal/mol, interacting with key residues involved in substrate recognition and activity modulation, such as GlyA20, ArgA14, and ThrC19. Compound NO-1, with a binding energy of –7.4 kcal/mol and substantial hydrogen bonding with GlyA18, GlyC18, ThrC19, MetC10, and ArgA14, demonstrates competitive or even superior affinity and interaction compared to these reference drugs, highlighting its strong antidiabetic potential.

For the anticancer target protein 3KOK, commonly used reference drug, imatinib[34], tend to display binding energies around –6.5 kcal/mol, with hydrogen bonds formed at residues critical for cancer pathway modulation such as LysA54, ValA92, and ArgA51. Compound NO-2, with a binding energy of –6.0 kcal/mol and multiple hydrogen bonds with ValA92, ArgA51, ThrA52, LysA54, and LeuA53, shows reasonable binding and selectivity, although slightly lower than the standard, yet its targeted interactions can still justify its selection for further anticancer studies.

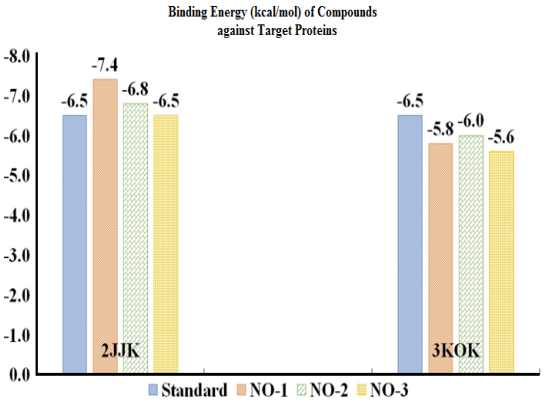

Fig. 7. Binding energy (Kcal/mol) of compounds against target proteins

When all three compounds are considered (Fig. 7), NO-1 stands out as the most effective antidiabetic agent based on its highest binding affinity (–7.4 kcal/mol) and extensive hydrogen bonding with key residues. NO-2, while less effective against the diabetic target, demonstrated the strongest anticancer activity (–6.0 kcal/mol) through multiple hydrogen bonds, reinforcing its candidacy for anticancer research. NO-3 displayed weaker interactions in both categories, suggesting limited therapeutic potential compared to NO-1 and NO-2.

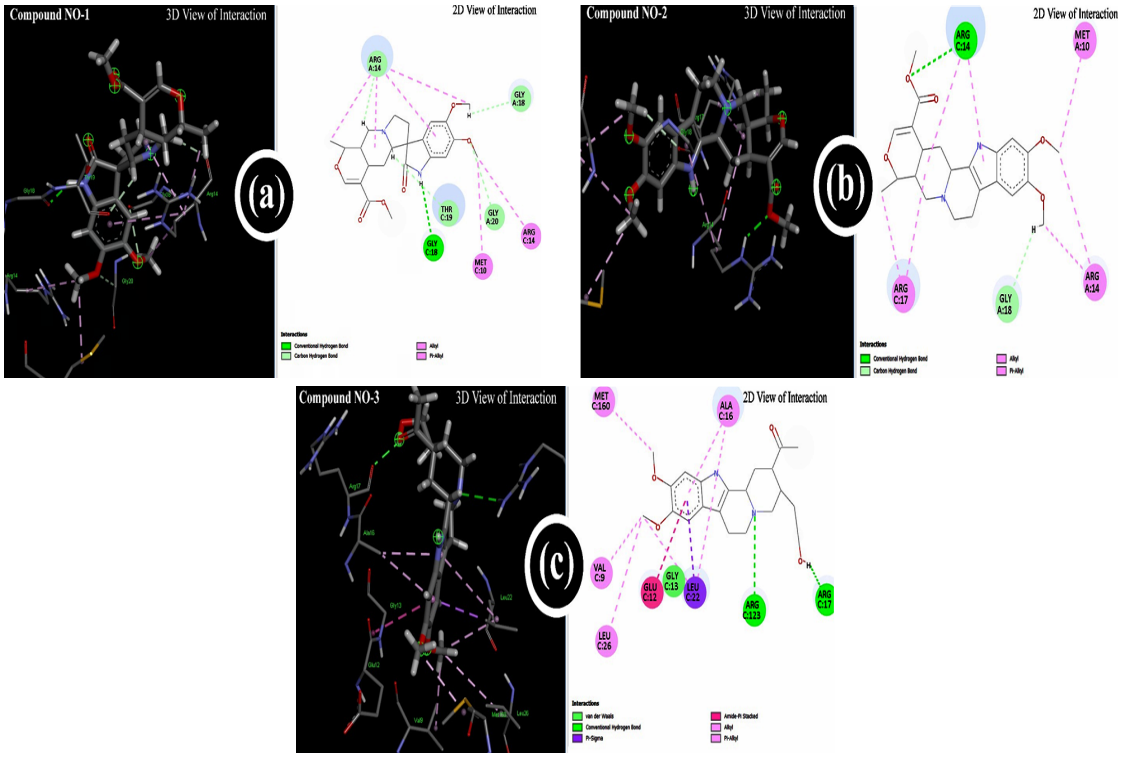

Fig. 8. Molecular docking results of (a) Compound NO-1 (b) Compound NO-2 (c) Compound NO-3 against fructose-1,6-bisphosphatase (FBPase, PDB ID: 2JJK) protein for anti-diabetic activity

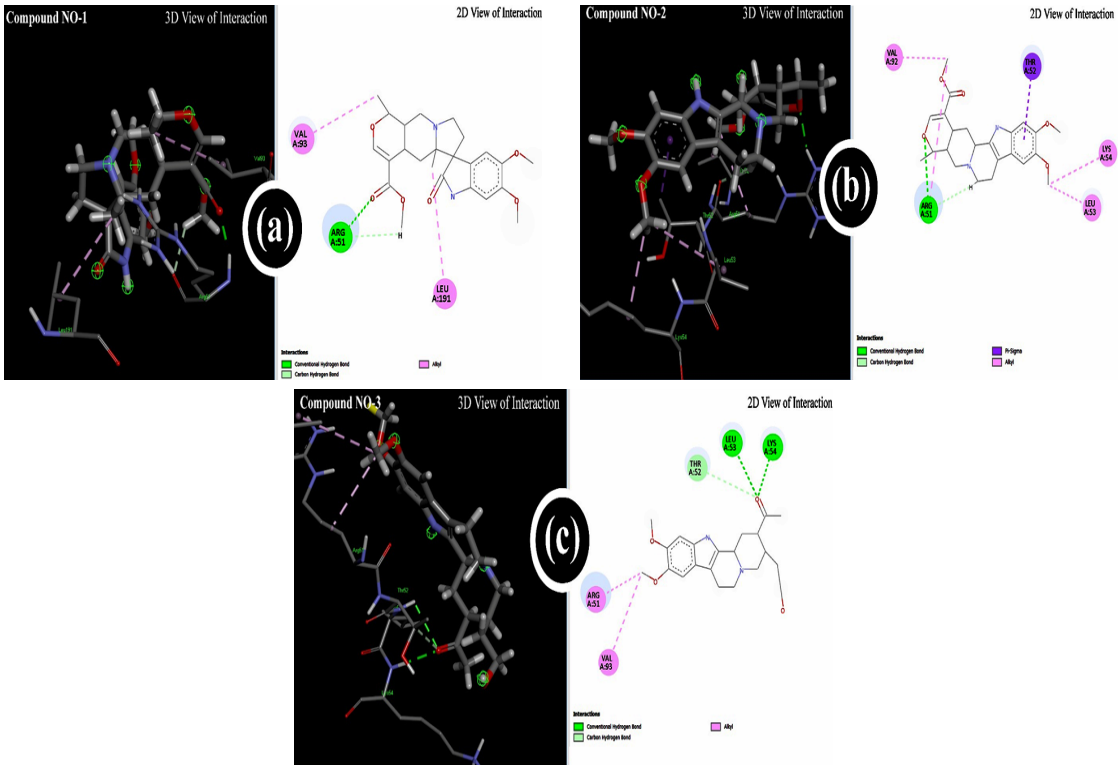

Fig. 9. Molecular docking results of (a) Compound NO-1 (b) Compound NO-2 (c) Compound NO-3 against phosphoinositide 3-kinase (PI3K, PDB ID: 3KOK) protein for anti-cancer activity

CONCLUSION

This study successfully isolated and characterized three indole alkaloids from Neisosperma oppositifolium leaf extract using maceration, Thin layer and column chromatography. Structural elucidation was confirmed by ATR-FTIR, ^{1}H NMR, ^{13}C NMR, and ESI-MS. *In-silico* evaluation predicted significant anti-diabetic and anti-cancer activities, with compound NO-1and NO-2 showing the highest activities. These findings support further *in-vitro* and *in-vivo* studies to validate the therapeutic potential of *N. oppositifolium* in modern drug development. Despite promising docking and *in silico* results, this study has key limitations. The stereochemical configurations of the isolated compounds require further confirmation through techniques such as NOE experiments and X-ray crystallography to fully determine their structures and better understand their biological significance. Moreover, the predicted bioactivities remain unverified as this study lacks experimental biological validation. Future research must include comprehensive *in vitro* and *in vivo* testing to assess both efficacy and safety. In addition, investigating pharmacokinetics and toxicity is crucial before these compounds can be considered for therapeutic use.

ACKNOWLEDGMENT

The authors would like to thank all contributors and reviewers whose invaluable insights and expertise greatly enhanced the quality of this manuscript.

Conflict of interest

The authors declare that they have no competing financial interests.

REFERENCES

1. Mushtaq, S.; Abbasi, BH.; Uzair, B.; Abbasi, R., *EXCLI J.*, **2018**, *17*, 420-451.
2. Shahid, RK.; Ahmed, S.; Le, D.; Yadav, S., *Cancers.*, **2021**, *13*, 5735.
3. Sun, H.; Saeedi, P.; Karuranga, S.; Pinkepank, M.; Ogurtsova, K.; Duncan, BB.; Stein, C.; Basit, A.; Chan, JCN.; Mbanya, JC.; Pavkov, ME.; Ramachandaran, A.; Wild SH.; James, S.; Herman, WH.; Zhang, P.; Bommer, C.; Kuo S.; Boyko, EJ.; Magliano, DJ., *Diab Res Clin Pract.*, **2022**, *183*, 109119.

4. Hossain, MJ.; Al-Mamun, M; Islam, MR., *Health Sci Rep*., **2024**, *7*, e2004.
5. Dilworth, L.; Facey, A.; Omoruyi, F., *Int. J. Mol. Sci.,* **2021**, *22*, 7644.
6. Sathishkumar, K.; Chaturvedi, M.; Das, P.; Stephen, S.; Mathur, P., *Indian J Med Res*., **2022**, *156*, 598-607.
7. Zhu, B.; Qu, S., *Front Endocrinol (Lausanne)*., **2022**, *13*, 800995.
8. Hirsch, I.B.; Juneja, R.; Beals, J.M.; Antalis, C.J.; E Wright, E., *Endocr. Rev*., **2020**, *41*, 733–755.
9. Nasim, N,; Sandeep, I.S,; Mohanty, S., *Nucleus*., **2022**, *65*, 399-411.
10. Qin, R.; You, FM.; Zhao, Q.; Xie, X.; Peng, C.; Zhan, G.; Han B., *J Hematol Oncol*., **2022**, *15*, 133.
11. Singh, P.; Singh, DP.; Patel, MK.; Binwal, M.; Kaushik, A.; Mall, M.; Sahu, M.; Khare, P.; Shanker, K.; Bawankule, DU.; Sundaresan, V.; Mani, DN.; Shukla, AK., *Protoplasma*., **2025**, *262*, 667-681.
12. Albin, BK.; Fred, JM.; Marvin, HM., *J Pharm. Sci*., **1972**, *61*, 1202-1205.
13. Alan, SC.; Norman, SS.; Howard, L., *Ann Intern Med*., **1959**, *51*, 238-247.
14. Deepanshi, T.; Mamta T., *Int. J. Pharmacogn. Life Sci*., **2020**, *1*, 38-43.
15. Youssef, T.; Jeremy K., *Elsevier*., **2015**, 118-197.
16. Yu, HI.; Chang, HY.; Lu, CH.; Tai, TS.; Kung, FP.; Zhang, YS.; Chang, YP.; Li, YZ.; Chen, SH.; Huang, JS.; Lee, YR., *Am J Cancer Res*., **2024**, *14*, 4989-4999.
17. Nurcahyanti, ADR.; Jap, A.; Lady, J.; Prismawan, D.; Sharopov, F.; Daoud, R.; Wink, M.; Sobeh, M., *Biomed. Pharmacother*., **2021**, *144*, 112138.
18. Chihomvu, P.; Ganesan, A.; Gibbons, S.; Woollard, K.; Hayes, MA., *Int J Mol Sci*., **2024**, *25*, 8792.
19. Divya, G.; Amina jega Y., *Results Chem*., **2025**, *14*, 102101.
20. Ponnusamy, N.; Pillai, G.; Arumugam, M., *J Biomol Struct Dyn*., **2023**, *42*, 3382–3395.
21. Alim Toraman, GO.; Senol, H.; Yazici Tutunis, S.; Tan, N.; Topcu, G., *Turk J Chem*., **2023**, *47*, 1260-1270.
22. Dubale, S.; Kebebe, D.; Zeynudin, A.; Abdissa, N.; Suleman, S., *J Exp Pharmacol*., **2023**, *15*, 51-62.
23. Dinesh, K.; Asheesh Kumar, G.; Navneet V.; Sushil Kumar., *Orient. J. Chem*., **2024**, *40*, 1127-1133.
24. Sarkar, PK.; Sarker, UK.; Farhana, F.; Md. Mahasin, Ali.; Md Atikul, Islamb.; Md. Azizul, Haquec.; Ishigamid, K.; Rokeyae, B.; Roy, B., *South African J. of Botany*., **2021**, *142*, 380-390.
25. Sultan, M.A.; Galil, M.S.A.; Al-Qubati, M.; Omar, M.M., *Barakat, A. Appl. Sci*., **2020**, *10*, 7727.
26. Paul D, van P.; Scott, CP.; Visvanathan, CC.; Bernard, RL.; Qun, D.; Mark, DE., *Diabetes.,* **2006**, *55*, 1747–1754.
27. Liu, P.; Cheng, H.; Roberts, TM.; Zhao, JJ., *Nat Rev Drug Discov*., **2009**, *8*, 627-644.
28. Johnson, T.O,; Adegboyega, A.E,; Ojo, O.A; Yusuf, A.J., *Front. Med*., **2022**, *9*, 907583.
29. Yusuf, A.J.; Adegboyega, A.E.; Yakubu, A.H.; Johnson, G.I., *Info. Med*., **2023**, *43*, 101406.
30. National Center for Biotechnology Information (**2025**). PubChem Compound summary for CID 67228, Reserpiline. Retrieved September 26, 2025 from https://pubchem.ncbi.nlm.nih.gov/compound/Reserpiline.
31. National Center for Biotechnology Information (**2025**). PubChem Compound Summary for CID 161345, Isoreserpiline. Retrieved September 26, 2025 from https://pubchem.ncbi.nlm.nih.gov/compound/Isoreserpiline.
32. National Center for Biotechnology Information (**2025**). PubChem Compound Summary for CID 6540753, Corynantheidine. Retrieved September 26, 2025 from https://pubchem.ncbi.nlm.nih.gov/compound/Corynantheidine.
33. Pedro, HOB.; Sonia, P.; Salete, JB.; Carlos, FGCG.; Batista, MT.; Maria MCS.; Artur, F., *J Ethnopharmacol*., **2021**, *280*, 114470.
34. V. Senthil Kumar, Ajay Kumar T V, V., *Parthasarathy. Curr. J. Appl. Sci. Technol.,* **2021**, *40*, 29-38.